

Inclusive $F(c\bar{s})$ hadroproduction

F. Hussain and K. Khan

Department of Physics, Quaid-i-Azam University, Islamabad, Pakistan

Sajjad Mahmood

International Centre for Theoretical Physics, Trieste, Italy

K. Rashid

Pakistan Institute of Nuclear Science and Technology, Rawalpindi, Pakistan

(Received 31 January 1984)

We present a leading-order perturbative QCD calculation of F -meson hadroproduction and evaluate the central and diffractive production cross sections at current ($E_{c.m.}=27.4$ GeV) and Tevatron (43.3 GeV) Fermilab energies.

I. INTRODUCTION

The hadroproduction of open charm is of considerable experimental and theoretical interest. Experimentally, these particles were observed to have unexpectedly large cross sections,¹ the mechanism of which was not understood for quite some time.² Further, it is of interest to note that the existence of all (e.g., Λ_c^+ and D) except the $F(c\bar{s})$ is well established. However, the F is expected to decay into $\nu_\tau + \tau$ 10–20 % of the time,³ and the decaying τ will produce an additional ν_τ , one of two yet-undiscovered members in the third lepton-quark generation. The most promising production reaction would involve the most energetic (Fermilab), most abundant (proton) beam in a fixed target.

Perturbative quantum chromodynamics (QCD) can be used to calculate open-charm production. QCD calculations for large-momentum-transfer inclusive processes employ factorization, which separates (short-distance) hard-scattering quark and gluon subprocesses from (large-distance) “soft” effects, which are incorporated in structure functions. To what extent this factorization can be justified is in itself an active area of research. We assume the validity of such a factorization.

We show that second-order diagrams contribute significantly to the hadroproduction of charm quarks. Quark-antiquark fusion is primarily responsible for central charm production (see Fig. 3), while some gluon-gluon annihilation processes⁴ demonstrate the non-Abelian character of QCD. Diffractive production, gluon-charm and quark-charm elastic scattering, provides the major part of the total cross section, and particularly so at large momentum transfers.

II. THE CALCULATION

We consider the inclusive process

$$p_A + p_B \rightarrow F^+ + x \quad (1)$$

shown in Fig. 1, where the F^+ has a momentum fraction transverse to the pp axis given by

$$x_T = 2p_F \sin\theta / (s)^{1/2}. \quad (2)$$

The momentum fraction parallel to the pp axis is

$$x_F = 2p_F \cos\theta / (s)^{1/2}, \quad (3)$$

where θ is the center-of-mass scattering angle, and the kinematic invariants are

$$s = (p_A + p_B)^2 = E_{c.m.}^2 \quad (4a)$$

$$t = (p_A - p_F)^2 = m_F^2 - E_{c.m.} \{ [m_F^2 + E_{c.m.} (x_F^2 + x_T^2)^{1/2}]^{1/2} + x_F/2 \} \quad (4b)$$

$$u = (p_B - p_F)^2 = m_F^2 - E_{c.m.} \{ [m_F^2 + E_{c.m.} (x_F^2 + x_T^2)^{1/2}]^{1/2} - x_F/2 \}, \quad (4c)$$

where m_F is the F^+ mass and we have chosen to neglect the proton mass.

The cross section for the process shown in Fig. 2, expressed in terms of the interaction cross section of the constituent partons (quarks and gluons), is generically

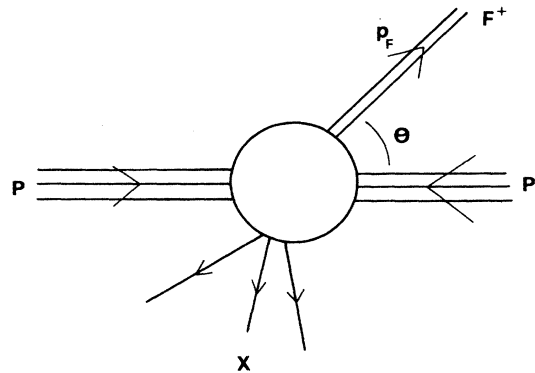


FIG. 1. Kinematics of the process $pp \rightarrow F^+ X$.

given as

$$\sigma = \int_0^1 \int_0^1 dx_a dx_b G_{a/A}(x_a, Q^2) G_{b/B}(x_b, Q^2) \times \hat{\sigma}(ab \rightarrow cd), \quad (5)$$

where x_a, x_b are the momentum fractions carried by the

interacting partons and $G_{a/A}, G_{b/B}$ specify the probability distributions of these partons in the colliding protons. Q^2 is the momentum transfer involved.

Accordingly, we write the differential cross section for the process $pp \rightarrow F^+ X$ as

$$E_F \frac{d\sigma}{d^3p_F} = \int \int \int dx_1 dx_2 dx_3^{-1} G_{a/p}(x_1, Q^2) G_{b/p}(x_2, Q^2) D_{c/F}(x_3) \frac{\hat{s}}{\pi} \delta(\hat{s} + \hat{t} + \hat{u} - 2m_c^2) \frac{d\hat{\sigma}}{d\hat{t}}(ab \rightarrow cd), \quad (6)$$

where x_1 and x_2 are the proton momentum fractions carried by a parton while x_3 is the fraction of c -quark momentum carried off by the F^+ . a, b, c , and d identify the interacting beam, target, charmed, and residue partons, respectively. The total differential cross section is found by summing over all subprocesses shown in Fig. 3. $G_{a/p}(x_i, Q^2)$ is the probability of finding a parton of type a with momentum fraction x_i in the proton at a particular Q^2 . The fragmentation function $D_{c/F}(x_3)$, is the probability that a charmed quark will constitute a F^+ which carries a fraction x_3 of its momentum, and is taken to be a constant in Q^2 here.

Using the subprocess invariants

$$\hat{s} = x_1 x_2 s,$$

$$\hat{t} = m_c^2 + x_1 x_3^{-1}(t - m_F^2), \quad (7)$$

$$\hat{u} = m_c^2 + x_2 x_3^{-1}(u - m_F^2),$$

we rewrite the differential cross section as

$$E_F \frac{d\sigma}{d^3p_F} = \int_0^1 \int_0^1 dx_1 dx_2 G_{a/p}(x_1, Q^2) G_{b/p}(x_2, Q^2) D_{c/F}(x_3) x_1 x_2 \left\{ (s/\pi) [x_1(t - m_F^2) + x_2(u - m_F^2)] \right\} \frac{d\hat{\sigma}(ab \rightarrow cd)}{d\hat{t}}, \quad (8)$$

where

$$x_3 = -[x_1(t - m_F^2) + x_2(u - m_F^2)]/x_1 x_2 s. \quad (9)$$

The region of x_1 and x_2 integration is constrained further due to the allowed region for \hat{t} , these kinematic constraints are⁵

$$[x_1 x_b / (x_1 - x_a)] < x_2 < 1, \quad (10a)$$

$$x_a / (1 - x_b) < x_1 < 1, \quad (10b)$$

where

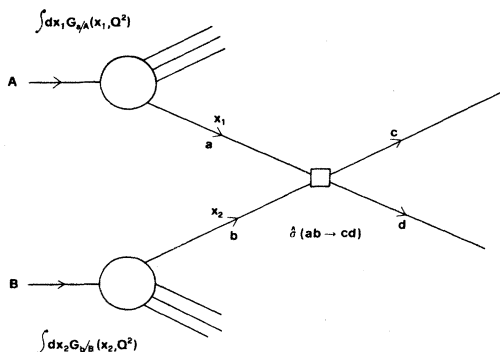


FIG. 2. A parton subprocess in a nucleon-nucleon interaction.

$$x_a = [x_F + (x_F^2 + x_T^2)^{1/2}]/2, \quad (11a)$$

$$x_b = [-x_F + (x_F^2 + x_T^2)^{1/2}]/2. \quad (11b)$$

The subprocess contributions of Fig. 3 are conveniently written as⁶

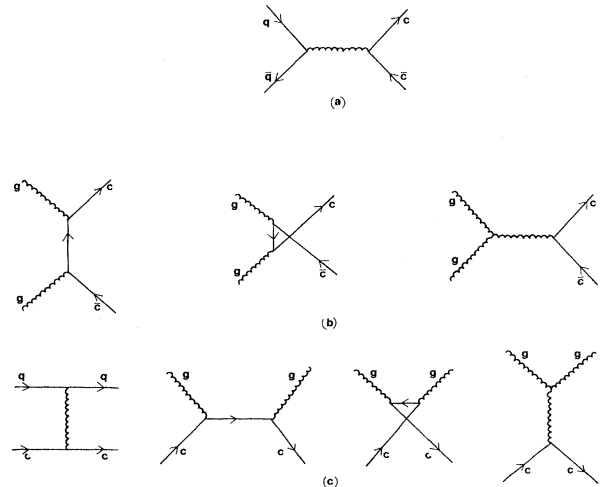


FIG. 3. Second-order subprocesses for charm-quark production in hadron-hadron collisions. (a) Quark-antiquark fusion, (b) gluon annihilation, and (c) quark-charm and gluon-charm diffractive graphs.

$$\begin{aligned}
\frac{d\hat{\sigma}}{d\hat{t}}(q\bar{q} \rightarrow c\bar{c}) &= \left[\frac{\hat{\sigma}_0}{3\hat{s}} \right] A(\hat{s}, \hat{t}, \hat{u}), \\
\frac{d\hat{\sigma}}{d\hat{t}}(gg \rightarrow c\bar{c}) &= \left[\frac{3\hat{\sigma}_0}{64\hat{s}} \right] B(\hat{s}, \hat{t}, \hat{u}), \\
\frac{d\hat{\sigma}}{d\hat{t}}(qc \rightarrow qc) &= \left[\frac{\hat{\sigma}_0}{3y_0} \right] A(\hat{t}, \hat{s}, \hat{u}), \\
\frac{d\hat{\sigma}}{d\hat{t}}(gc \rightarrow gc) &= \left[\frac{-\hat{\sigma}_0}{8y_0} \right] B(\hat{t}, \hat{s}, \hat{u}),
\end{aligned} \tag{12}$$

with

$$\begin{aligned}
A(\alpha, \beta, \gamma) &= \frac{\beta'^2 + \gamma'^2 - 2m_c^2 \alpha}{\alpha^2}, \\
B(\alpha, \beta, \gamma) &= \left[\frac{12\beta'\gamma'}{\alpha^2} - \frac{2}{3} \frac{m_c^2 \alpha''}{\beta'\gamma'} \right] \\
&\quad + \left[\left[\frac{8}{3} \frac{\beta'\gamma' - 2m_c^2(m_c^2 + \beta)}{\beta'^2} \right. \right. \\
&\quad \left. \left. - 6 \frac{\beta'\gamma' + m_c^2(\gamma - \beta)}{\alpha\beta'} \right] \right. \\
&\quad \left. + (\beta \leftrightarrow \gamma, \beta' \leftrightarrow \gamma') \right],
\end{aligned} \tag{13}$$

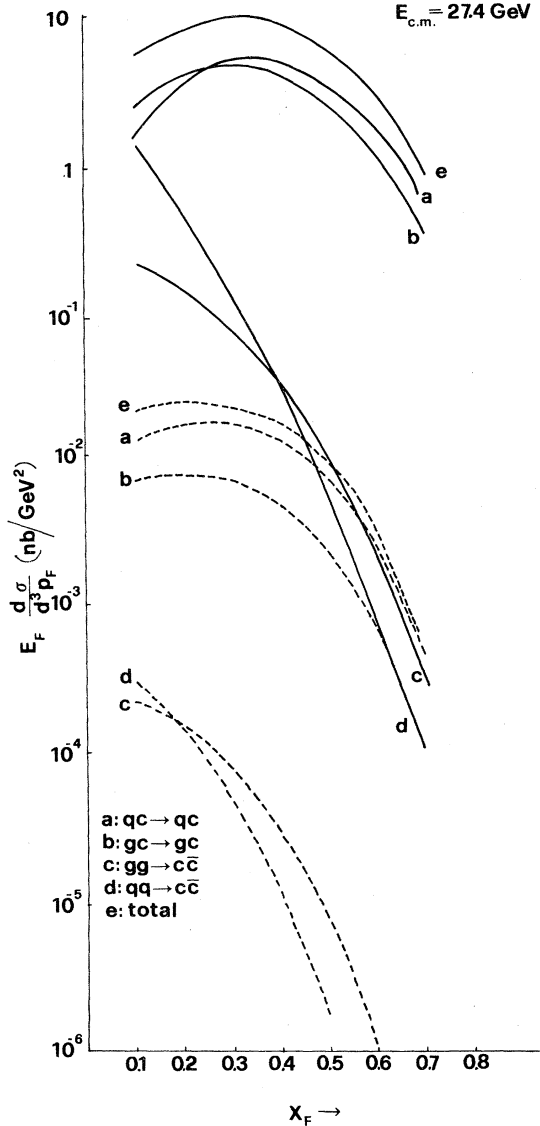


FIG. 4. Subprocess and total differential cross section versus longitudinal momentum fraction at $E_{c.m.} = 27.4$ GeV. Dashed curves refer to $x_T = 0.3$ while full curves are for $x_T = 0.1$.

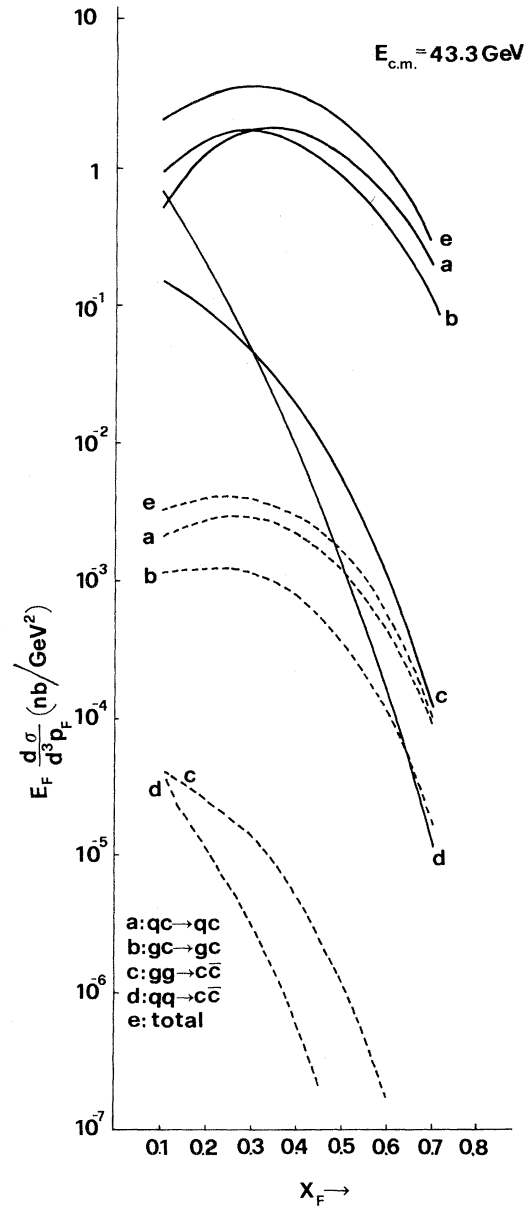


FIG. 5. Subprocess and total differential cross sections versus x_F at $E_{c.m.} = 43.3$ GeV. Dashed curves are for $x_T = 0.3$, full curves are for $x_T = 0.1$.

where

$$\beta' \equiv (m_c^2 - \beta), \quad \gamma' \equiv (m_c^2 - \gamma), \quad \alpha'' \equiv (\alpha - 4m_c^2) \quad (14)$$

and

$$\hat{\sigma}_0 = \frac{4\pi\alpha_s^2}{3\hat{s}}, \quad y_0 = (\hat{s} - m_c^2)^2 / \hat{s}. \quad (15)$$

The strong coupling strength α_s is

$$\alpha_s(Q^2) = \frac{12\pi}{25 \ln(Q^2/\Lambda^2)}, \quad (16)$$

where Q^2 the momentum transfer is calculated as

$$Q^2 = \frac{2\hat{u}\hat{t}\hat{s}}{(\hat{u}^2 + \hat{t}^2 + \hat{s}^2)}. \quad (17)$$

We take $\Lambda = 0.5$ GeV, $m_c = 1.4$ GeV, and $m_F = 1.8$ GeV.

III. THE FRAGMENTATION AND DISTRIBUTION FUNCTIONS

The other main ingredients of a perturbative QCD calculation such as the present one are the fragmentation and

distribution functions. The fragmentation function $D_{c/F}$ implied from e^+e^- inclusive data⁷ is

$$D_{c/F}(x) \sim (1-x)^n, \quad 0 \leq n \leq 1, \quad (18)$$

normalized using the flavor-momentum sum rule,

$$\sum_{n'} \int_0^1 x D_{q/n'}(x) dx = 1. \quad (19)$$

Because noncharm-meson production requires the creation of a $c\bar{c}$ pair in a vacuum which is suppressed due to the large charm-quark mass, we assume that only the charmed pseudoscalar mesons are produced by the c quark. Further, we assume

$$D_{c/D^+} = D_{c/D^0} = D_{c/F^+} \quad (20a)$$

so that

$$D_{c/F^+}(x) = 2(1-x) \quad \text{for } n=1, \quad (20b)$$

which is lower than Feynman-Field⁸ by about 20%.

In considering the distribution of charm in the proton, $G_{c/p}$, we ignore the intrinsic charm contribution.⁹ We take the charm to be generated by the QCD evolution of the structure functions: at low Q^2 the proton's charm content is undetectable but at $Q^2 \geq 4m_c^2$ there is sufficient resolution to find the c quark deep inside the proton.

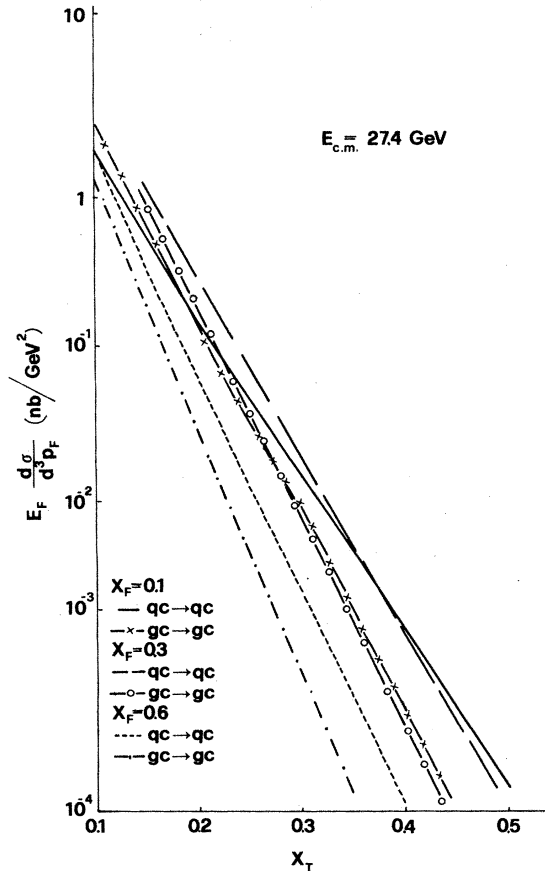


FIG. 6. Diffractive subprocess cross sections versus x_T at $E_{c.m.} = 27.4$ GeV.

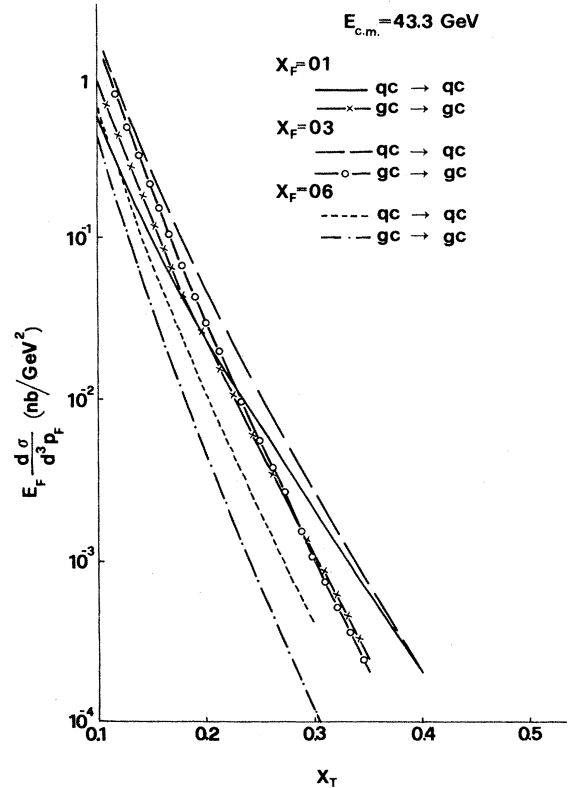


FIG. 7. Diffractive subprocess cross sections versus x_T at $E_{c.m.} = 43.3$ GeV.

Hence, to evaluate the flavor-excitation cross section we take as the QCD-evolved charm distribution^{2,3,9}

$$G_{c/p}(x, \langle Q^2 \rangle) = Nx^{l-1}(1-x)^k \quad (21a)$$

at an effective average value $\langle Q^2 \rangle$. The normalization constant N is fixed by the result

$$\int_0^1 dx x G_{c/p}(x) = 0.005, \quad (21b)$$

which is the level of charm found at $Q^2 = 4m_c^2$ in a QCD moment analysis.¹⁰ The parameters l and k are chosen to be $\geq \frac{1}{2}$ so that $xG_{c/p}(x)$ resembles the momentum distribution of the valence quarks. For $l=k=3$ we find

$$G_{c/p}(x) = 0.70x^2(1-x)^3. \quad (22)$$

For the valence quarks, in a proton we shall use counting-rulelike input distributions at $Q^2 = Q_0^2$. The

parametrizations suggested by Buras and Gaemers^{10,11} are followed as regards the Q^2 dependence of nucleonic distributions.

The sea and gluon distributions along with their Q^2 distribution have been worked out by Mellen inverting the appropriate moments predicted by QCD. We use the parametrization given by Owens and Reya.¹¹

IV. RESULTS

For the subprocesses of Eq. (12) we evaluate the differential cross section [Eq. (6)]. In Figs. 4 and 5 we show the results over a range $0.1 \leq x_F \leq 0.8$ at different fixed transverse momentum fractions x_T . The plots are for center-of-mass energies of 27.4 and 48.3 GeV corresponding to proton beam energies of 400 and 1000 GeV. As is clear, the major contributions to F^+ production come from gluon- and quark-charm diffractive scattering which exhibit a maxima around $x_F = 0.2-0.3$ at $x_T = 0.1$, which shifts to lower x_F as we go to $x_T = 0.3$. The contributions of the $q\bar{q}$ fusion and gluon-gluon annihilation graphs are appreciable only for small x_F , x_T , and fall rapidly with increasing x_F and x_T .

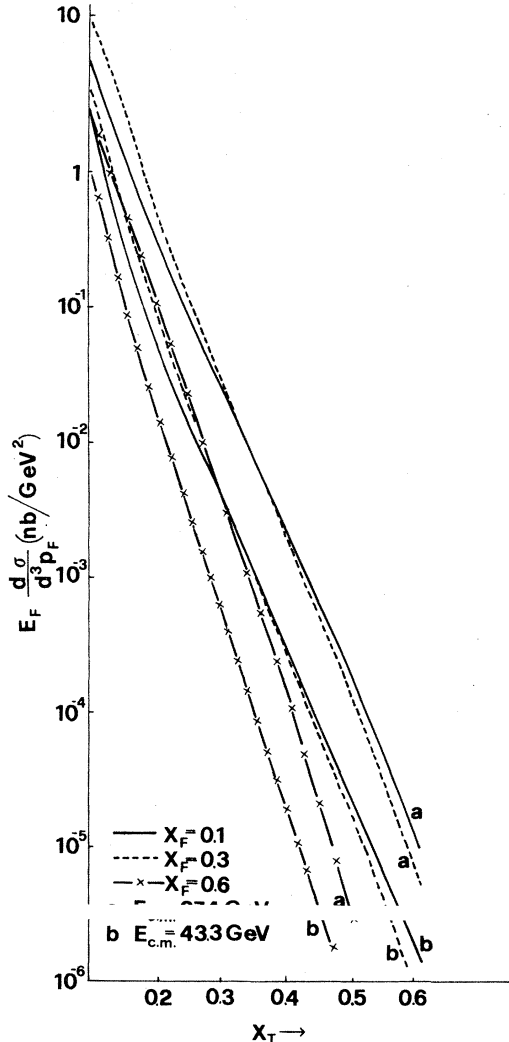


FIG. 8. Total differential cross section versus x_T . (a) $E_{c.m.} = 27.4$ GeV. (b) $E_{c.m.} = 43.3$ GeV.

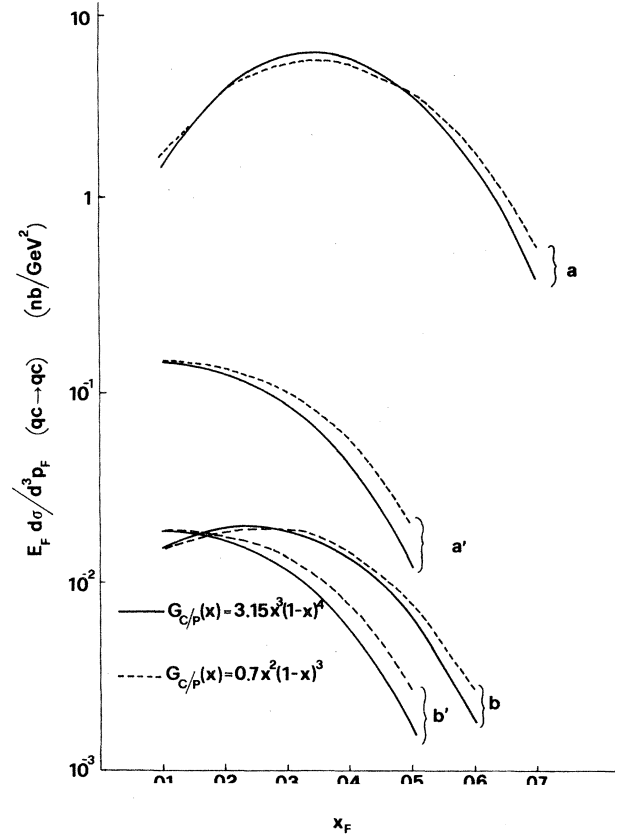


FIG. 9. Diffractive subprocess cross section ($qc \rightarrow qc$) vs x_F for different charm-quark distributions. a and a' refer to $E_{c.m.} = 27.4$ GeV, and b and b' to $E_{c.m.} = 43.3$ GeV. For a' and b' , $x_T = 0.5$ and the scale is to be multiplied by 10^{-3} , whereas a and b are at $x_T = 0.1$.

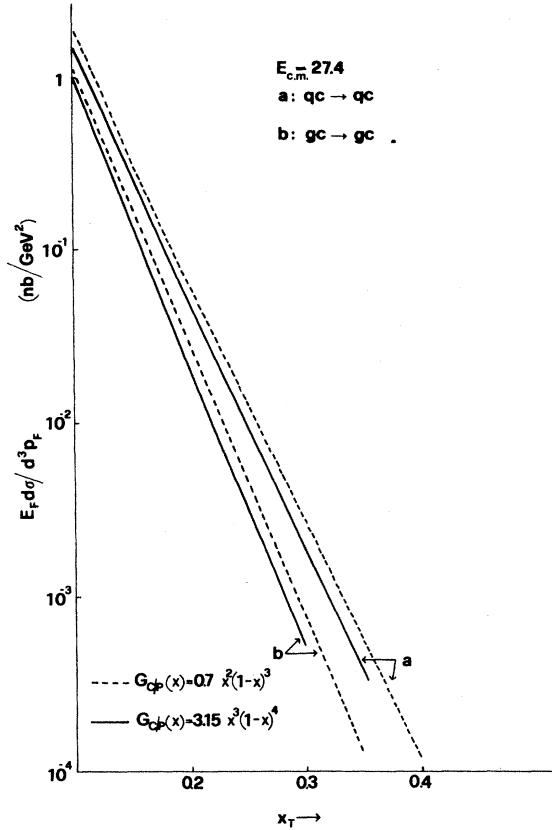


FIG. 10. Subprocess cross sections versus x_T for $x_F=0.1$ and different charm distributions.

In Figs. 6 and 7 we plot the x_T dependence of the diffractive subprocesses involved. The fusion contributions drop even more sharply, and diffractive subprocesses are expected to dominate, as is also clear from Figs. 4 and 5,

and Fig. 8 which plots the fall of the total cross section with rising x_T .

Thus, we note that the diffractive production of charm can explain the large observed cross sections.¹² Further, one can expect the forward x_F region to be a good place to search for heavier flavors, such as b and t .

In order to investigate the dependence of our calculation on the particular choice of charm distribution [Eq. (22)], we have repeated calculations of qc and gc subprocesses using a softer charm distribution,

$$G_{c/p}(x) = 3.15x^3(1-x)^4. \quad (23)$$

The results are plotted in Figs. 9 and 10. Figure 9 compares predictions for $qc \rightarrow qc$ subprocess for the two charm distributions used [Eqs. (22) and (23)]. The difference becomes significant for large x_F and x_T . Similarly the plot, Fig. 10, for x_T dependence of these diffractive subprocesses exhibits small differences which, however, are not essential for a qualitative understanding.

ACKNOWLEDGMENTS

We would like to thank W. P. Trower for suggesting the study of F^+ production and for providing the VEGAS Monte Carlo integration program used in the calculation. The authors are also grateful to N. S. Craigie for suggestions and useful discussions. S. M. also gratefully acknowledges support from Centre for Basic Sciences, Islamabad, Pakistan. One of the authors (S.M.) would like to thank Professor Abdus Salam, the International Atomic Energy Agency, and UNESCO for hospitality at the International Centre for Theoretical Physics, Trieste.

- ¹R. J. N. Phillips, in *High Energy Physics—1980*, proceedings of the XXth International Conference, Madison, Wisconsin, edited by L. Durand and L. G. Pondrom (AIP, New York, 1981), p. 1470; see also S. Wojcicki, *ibid.*, p. 1430.
- ²V. Barger, F. Halzen, and W. Y. Keung, *Phys. Rev. D* **25**, 112 (1982).
- ³V. Barger, J. P. Leveille, P. M. Stevenson, and R. J. N. Phillips, *Phys. Rev. Lett.* **45**, 83 (1980).
- ⁴M. Glück, J. F. Owens, and E. Reya, *Phys. Rev. D* **17**, 2324 (1978).
- ⁵N. Fleishon and W. J. Stirling, *Nucl. Phys.* **B188**, 205 (1981).
- ⁶B. L. Combridge, *Nucl. Phys.* **B151**, 429 (1979); see also Ref. 2 where in $A(\alpha, \beta, \gamma)$ one power of β' and γ' is missing.
- ⁷A. Ali, J. G. Körner, and G. Kramer, *Nucl. Phys.* **B18**, 409 (1980); R. Odorico, *Phys. Lett.* **71B**, 121 (1977); and K. Berk-

- elman, in *Proceedings of the 19th International Conference on High Energy Physics, Tokyo, Japan, 1978*, edited by S. Homma, M. Kawaguchi, and H. Miyazawa (Phys. Soc. of Japan, Tokyo, 1979).
- ⁸R. D. Field and R. P. Feynman, *Nucl. Phys.* **B136**, 1 (1978); R. P. Feynman, R. D. Field, and G. C. Fox, *Phys. Rev. D* **18**, 3320 (1978).
- ⁹S. J. Brodsky, P. Hoyer, C. Peterson, and N. Sakai, *Phys. Lett.* **93B**, 451 (1980); S. J. Brodsky, C. Peterson, and N. Sakai, *Phys. Rev. D* **23**, 2745 (1981).
- ¹⁰A. J. Buras and K. J. F. Gaemers, *Nucl. Phys.* **B132**, 249 (1978).
- ¹¹J. Owens and E. Reya, *Phys. Rev. D* **17**, 3003 (1978).
- ¹²R. Odorico, *Nucl. Phys.* **B209**, 77 (1982).